Arteriosclerosis, Thrombosis, and Vascular Biology

TRANSLATIONAL SCIENCES

# Differential Impact In Vivo of Pf4-ΔCre–Mediated and Gp1ba-ΔCre–Mediated Depletion of Cyclooxygenase-1 in Platelets in Mice

Soon Yew Tang, Ronan Lordan, Hu Meng, Benjamin J. Auerbach, Elizabeth J. Hennessy, Arjun Sengupta, Ujjalkumar S. Das, Robin Joshi, Oscar A. Marcos-Contreras, Ryan McConnell, Gregory R. Grant, Emanuela Ricciotti, Vladimir R. Muzykantov, Tilo Grosser, Aalim M. Weiljie, Garret A. FitzGerald

**BACKGROUND:** Low-dose aspirin is widely used for the secondary prevention of cardiovascular disease. The beneficial effects of low-dose aspirin are attributable to its inhibition of platelet Cox (cyclooxygenase)-1–derived thromboxane $A_2$. Until recently, the use of the Pf4 (platelet factor 4) Cre has been the only genetic approach to generating megakaryocyte/platelet ablation of Cox-1 in mice. However, Pf4-ΔCre displays ectopic expression outside the megakaryocyte/platelet lineage, especially during inflammation. The use of the Gp1ba (glycoprotein 1bα) Cre promises a more specific, targeted approach.

**METHODS:** To evaluate the role of Cox-1 in platelets, we crossed Pf4-ΔCre or Gp1ba-ΔCre mice with Cox-$1^{flox/flox}$ mice to generate platelet Cox-$1^{-/-}$ mice on normolipidemic and hyperlipidemic ($Ldlr^{-/-}$; low-density lipoprotein receptor) backgrounds.

**RESULTS:** Ex vivo platelet aggregation induced by arachidonic acid or adenosine diphosphate in platelet-rich plasma was inhibited to a similar extent in Pf4-ΔCre Cox-$1^{-/-}$/$Ldlr^{-/-}$ and Gp1ba-ΔCre Cox-$1^{-/-}$/$Ldlr^{-/-}$ mice. In a mouse model of tail injury, Pf4-ΔCre–mediated and Gp1ba-ΔCre–mediated deletions of Cox-1 were similarly efficient in suppressing platelet prostanoid biosynthesis. Experimental thrombogenesis and attendant blood loss were similar in both models. However, the impact on atherogenesis was divergent, being accelerated in the Pf4-ΔCre mice while restrained in the Gp1ba-ΔCres. In the former, accelerated atherogenesis was associated with greater suppression of $PGI_2$ biosynthesis, a reduction in the lipopolysaccharide-evoked capacity to produce $PGE_2$ (prostaglandin E) and $PGD_2$ (prostanglandin D), activation of the inflammasome, elevated plasma levels of IL-1β (interleukin), reduced plasma levels of HDL-C (high-density lipoprotein receptor-cholesterol), and a reduction in the capacity for reverse cholesterol transport. By contrast, in the latter, plasma HDL-C and α-tocopherol were elevated, and MIP-1α (macrophage inflammatory protein-1α) and MCP-1 (monocyte chemoattractant protein 1) were reduced.

**CONCLUSIONS:** Both approaches to Cox-1 deletion similarly restrain thrombogenesis, but a differential impact on Cox-1–dependent prostanoid formation by the vasculature may contribute to an inflammatory phenotype and accelerated atherogenesis in Pf4-ΔCre mice.

**GRAPHIC ABSTRACT:** A graphic abstract is available for this article.

**Key Words:** atherosclerosis ■ blood platelets ■ cyclooxygenase-1 ■ hemostasis ■ thrombosis



Randomized controlled trials have provided evidence that low-dose aspirin is effective in the secondary prevention of cardiovascular diseases.[1] In patients who have previously experienced a heart attack or stroke, the cardiovascular benefit of low-dose aspirin exceeds the risk of gastrointestinal bleeding. The place of low-dose aspirin in primary prevention remains controversial.[1,2] For example, a recent randomized controlled trial in patients with diabetes showed that low-dose aspirin reduced serious vascular events but caused major bleeding events that offset this benefit.[3] While inhibition of platelet thromboxane $A_2$ is sufficient to explain

Correspondence to: Garret A. FitzGerald, MD, Institute for Translational Medicine and Therapeutics, Perelman School of Medicine, 10-110 Smilow Center for Translational Research, University of Pennsylvania, 3400 Civic Center Blvd, Bldg 421, Philadelphia, PA 19104. Email garret@upenn.edu
Supplemental Material is available at https://www.ahajournals.org/doi/suppl/10.1161/ATVBAHA.123.320295.
For Sources of Funding and Disclosures, see page 1405.

*Arterioscler Thromb Vasc Biol* is available at www.ahajournals.org/journal/atvb

## Nonstandard Abbreviations and Acronyms

| | |
|---|---|
| **AA** | arachidonic acid |
| **Abc** | ATP binding cassette |
| **Bpifa1** | bacterial permeability family member A1 |
| **Cox** | cyclooxygenase |
| **Gp1ba** | glycoprotein 1bα |
| **HFD** | high-fat diet |
| **Igha** | immunoglobulin heavy chain a |
| **MCP-1** | monocyte chemoattractant protein 1 |
| **MIP-1α** | macrophage inflammatory protein-1α |
| **Pf4** | platelet factor 4 |
| **PGIM** | 2,3-dinor 6-keto $PGF_{1\alpha}$ |
| **Scgb1a1** | secretoglobin family 1A member 1 |
| **Scgb3a1** | secretoglobin family 3A member 1 |
| **Scgb3a2** | secretoglobin family 3A member 2 |
| **scRNA-seq** | single-cell RNA sequencing |
| **TxM** | 2,3-dinor $TxB_2$ |

the clinical effects of low-dose aspirin, aspirin has other effects on thrombus formation unrelated to the inhibition of platelet Cox (cyclooxygenase)-1 activity.[2,4] Aspirin also mimics some of the effects of caloric restriction.[5] The availability of genetic models of Cox-1 ablation in megakaryocyte/platelets facilitates elucidation of the relative importance of these observations.

The first available model utilized Pf4 (platelet factor 4) ΔCre–mediated recombination. However, this is not limited to the megakaryocyte/platelet lineage, especially during inflammation.[6,7] Pf4-ΔCre–mediated deletion of Cox-1 in megakaryocyte/platelets ameliorates dextran sulfate sodium–induced colitis in mice and prolongs the time to occlusion in the carotid artery in a mouse model of $FeCl_3$-induced thrombosis.[8,9] More recently, Nagy et al[6] developed a transgenic mouse model in which Cre expression is driven by the Gp1ba (glycoprotein 1bα) locus, which is more specific to megakaryocyte/platelets than the Pf4-ΔCre transgenic mouse. However, recombination may be less efficient than in Pf4-ΔCre mice, and the introduction of Cre through constitutive knock-in results in heterozygous deletion of GP1ba, which itself may modify the platelet phenotype. The authors advocated Cre to be used as the control for conditional deletion using Pf4-ΔCre–mediated and Gp1ba-ΔCre–mediated recombination. Gollomp and Poncz[10] summarized what is known about the 2 models and suggested that they should be compared to assess their comparative impact on platelet biology in vivo.

Here, we directly compared the effects of Pf4-ΔCre–mediated or Gp1ba-ΔCre–mediated deletion of Cox-1 in platelets on ex vivo platelet aggregation, prostanoid biosynthesis, hemostasis, thrombosis, and atherosclerosis.

## Highlights

- A direct evaluation of the impact of Cox-1 depletion in platelets mediated by Pf4 (platelet factor 4)-ΔCre or Gp1ba (glycoprotein 1bα)-ΔCre on prostanoid biosynthesis and models of cardiovascular disease.
- Ex vivo platelet aggregation, platelet prostanoid biosynthesis, experimental thrombogenesis, and hemostasis are equally impacted in both models.
- The effect of platelet Cox-1 depletion on atherogenesis is divergent; it is accelerated in the Pf4-ΔCre mice while restrained in the Gp1ba-ΔCre mice.
- The divergent atherogenic phenotypes may be attributable to the differential impact on atheroprotective prostanoids and inflammation from Cox-1 depletion in platelets mediated by Pf4-ΔCre versus Gp1ba-ΔCre.

# MATERIALS AND METHODS

## Data Availability

The authors declare that all supporting data are available within the article (and its Supplemental Material). Supplemental Material includes resources available from the corresponding author upon reasonable request.

All reagents used were purchased from MilliporeSigma (St. Louis, MO) unless otherwise stated. A detailed description of the experimental methods is provided in the Supplemental Methods.

All animals in this study were housed according to the guidelines of the Institutional Animal Care and Use Committee of the University of Pennsylvania. Animals that developed skin lesions during the feeding of a high-fat diet were excluded. All experimental protocols were approved by the Institutional Animal Care and Use Committee (protocol number 804754).

## Animals Studies

Platelet-specific Cox-1–deficient mice were generated by crossing male Pf4-ΔCre or Gp1ba-ΔCre mouse lines with female Cox-$1^{flox/flox}$ mice, as described in the Supplemental Methods.

## Isolation of Platelets and Primary Megakaryocytes From Hyperlipidemic Mice ($Ldlr^{-/-}$)

Blood was centrifuged at 200*g* for 10 minutes at room temperature to obtain platelet-rich plasma. Platelets were obtained from platelet-rich plasma by centrifuging at 3000*g* for 10 minutes at room temperature.

Mature primary megakaryocytes were isolated from bone marrows (femora and tibiae) by size exclusion via filtration as reported by Spindler et al.[11]

## Ex Vivo Platelet Aggregation Assay

Platelet aggregation in response to adenosine diphosphate and arachidonic acid (AA) was measured using optical multichannel

(optimul) platelet aggregometry in 96-well plates, as described by Chan et al.[12]

## Platelet Activation by Tail Injury in Normolipidemic Mice

Two millimeters of tail was amputated using a sterile scalpel under anesthesia with isoflurane. Urinary prostanoid metabolites and serum protanoids were measured using liquid chromatography/mass spectrometry/mass spectrometry.

## Mass Spectrometric Analysis of Urinary Prostaglandin Metabolites and Isoprostanes

Urinary prostanoid metabolites were measured by liquid chromatography/mass spectrometry/mass spectrometry as described.[13] Such measurements provide a noninvasive, time-integrated measurement of systemic prostanoid biosynthesis.[14]

## Mass Spectrometric Analysis of Serum and Cell Culture Media Prostanoids

Prostanoids in serum from mice and cell culture media of mouse aortas were measured, as described by Meng et al.[15]

## Blood Loss by Tail Amputation in Hyperlipidemic Mice (Ldlr$^{-/-}$)

Mice were used in this experiment after feeding a high-fat diet (HFD) for 12 weeks; 2 mm of the tail was amputated using a sterile scalpel under anesthesia with ketamine/xylazine/acepromazine. Blood was collected into a preweighed glass tube containing Drabkin reagent to estimate the amount of blood loss and hemoglobin content at 420 nm using a microplate reader.

## Photochemical Vascular Injury Induced Thrombosis in Female Hyperlipidemic Mice (Ldlr$^{-/-}$)

Briefly,[16] ≈14-week-old female mice were anesthetized and secured on a thermal pad at 37 °C. A midline cervical incision was made to locate the right common carotid artery, and a Doppler flow probe was applied. Rose Bengal (10 mg/mL) was injected into the jugular vein of a mouse (50-mg/kg body weight), and a 1.5-mW green light laser (540 nm) was used to induce thrombosis. Blood flow was monitored for up to 90 minutes, and occlusion time was recorded when blood flow was reduced to zero for up to 1 minute.

## Laser-Induced Thrombus Formation and Intravital Microscopy in Male Hyperlipidemic Mice (Ldlr$^{-/-}$)

Briefly,[17] anesthetized male mice (12–16 weeks old) kept at 37 °C on a thermal pad were administrated intravenously with rat anti-mouse CD41 (20 µg/mL) and Alexa Flour 488 chicken anti-rat IgG (180 µg/mL) diluted in PBS. The cremaster muscle was exteriorized, pinned over the microscopy stage, and bathed in a bicarbonate-buffered saline at 37 °C. SlideBook 6.0 imaging software (Intelligent Imaging Innovations) was used to control all parts of the intravital microscope, data collection, and image analysis. Digital images of thrombus formation were obtained with an Olympus BX61WI microscope.

## Atherogenesis Study

Mice of both sexes on an Ldlr$^{-/-}$ (low-density lipoprotein receptor) background were fed an HFD (21.2% fat, 0.2% cholesterol, TD.88137; Harlan Teklad, Madison, WI) from 8 weeks of age for 12, 24, and 36 weeks. Body weights were recorded, and urine samples were collected from the mice before and after the HFD feeding.

## Single-Cell RNA Sequencing of Mouse Aortas and Analysis

Aortas (ascending aorta, aortic arch, descending aorta, innominate artery, carotid arteries, subclavian arteries, and descending aorta) of male Ldlr$^{-/-}$ mice fed an HFD for 24 weeks were dissected for single-cell isolation with a cocktail of enzymes (DNase, liberase, and hyaluronidase) in a petri dish at 37 °C for 40 minutes. Cell supernatant was filtered through a 40-µm strainer and washed with RPMI 1640 containing 10% fetal bovine serum to inactive the enzyme cocktail. Mouse aortas from 2 mice per group were pooled after enzymatic digestion for scRNA sequencing. For single-cell RNA sequencing (scRNA-seq) data cell quality control, cells were filtered for the presence of doublets using Scrublet.[18] After identifying cell types, a low-dimensional cell embedding was estimated using scVI.[19] Using the low-dimensional embedding, cells were then clustered using the Leiden algorithm[20] with resolution 0.2 type marker gene identification.

## Plasma Extraction for Metabolomics Study

Mouse plasma samples (50 µL) were extracted with 300-µL ice-cold methanol: chloroform solution (2:1). The top fraction was analyzed using Ultra Performance Liquid Chromatography–mass spectrometry/mass spectrometry as reported previously.[21] Data analysis was normalized with the probabilistic quotient normalization in R.[22]

## In Vivo Reverse Cholesterol Transport Assay

Bone marrow–derived macrophages were prepared from male C57Bl/6J mice, and a reverse cholesterol transport assay was performed as previously described.[23,24]

## Statistics

All animals compared were the stated age and some were on the same Ldlr$^{-/-}$ background (C57BL/6J). The residuals were tested for normality by the D'Agostino/Pearson test. Post hoc analysis was performed by pairwise *t* tests, with the Bonferroni correction unless otherwise stated. All significant tests were further validated by the nonparametric Mann-Whitney *U* and Wilcoxon tests to make sure that they were not biased by parametric assumption. A significance threshold of 0.05 was used for all tests after correcting for multiple tests. Sample sizes (10–20) were based on power analysis of the test measurement and the desire to detect a minimal 10% difference in the variables assessed with $\alpha$=0.05 and the power (1−$\beta$)=0.8.

For scRNA sequencing, to assess the differential expression of genes among the combinations of conditions, gene transcript counts were transformed as they were for all scRNA-seq analyses. Thereafter, a difference of means of each pair of transformed count distributions was assessed using a Mann-Whitney *U* test. Additional filtering was done by 2 further criteria. First, the effect size of the difference of means was estimated. Those with effect sizes ≥0.3 were kept. Second, the percentage of cells with detected expression was detected. Genes with at least 10% detected expression across cells in 1 of the 2 conditions were kept.

## RESULTS

### Pf4-ΔCre–Mediated or Gp1ba-ΔCre–Mediated Deletion of Platelet Cox-1 Reduces Cox-1 mRNA and Protein in Platelets and Megakaryocytes in Hyperlipidemic Mice (Ldlr$^{-/-}$) Fed a Standard Laboratory Diet

DNA extracted from the mouse tail was used to confirm the genotypes of our mouse models by polymerase chain reaction (PCR) analyses. PCR products of Pf4-ΔCre, Gp1ba-ΔCre, flox (flanking by LoxP), and Ldlr are 450, 372, 210, and 550 bp, respectively (Figure S1A). The excision product of the floxed Cox-1 gene resulted in a PCR product of 327 bp (Figure S1A, bottom).

Pf4-ΔCre–mediated or Gp1ba-ΔCre–mediated deletion of Cox-1 reduces Cox-1 mRNA and is shown in platelets and megakaryocytes isolated from platelet-rich plasma and bone marrow, respectively (Figure S1B and S1C). mRNA of glycoprotein IIb/IIIa integrin (CD41) was enriched in platelets and megakaryocytes. Platelet CD41 mRNA levels of Gp1ba-ΔCre control mice were significantly higher than in Pf4-ΔCre control mice. These results agree with the increase in platelet volume of the Gp1ba-ΔCre mouse model, as reported by Nagy et al.[6] Despite having different Cox-1 mRNA levels in the 2 Cre controls, Cox-1 mRNA and protein in platelets and megakaryocytes from Cox-1$^{-/-}$ mice were depleted to a similar extent after Cre-mediated recombination (Figure S1B and S1C). Consistent with this, serum $TxB_2$, $PGE_2$ (prostaglandin E), $PGD_2$ (prostanglandin D), and $PGF_{2\alpha}$ levels were significantly suppressed in both knockout lines (Figure S1D).

### Deletion of Platelet Cox-1 Inhibits Ex Vivo Platelet Aggregation Induced by AA or Adenosine Diphosphate

Platelet-rich plasma isolated from the whole blood of controls or platelet Cox-1$^{-/-}$ hyperlipidemic (Ldlr$^{-/-}$) mice fed a standard laboratory diet was used to perform a platelet aggregation assay using a microplate reader.

Deletion of Cox-1 in platelets from both lines significantly inhibited platelet aggregation induced with AA or adenosine diphosphate (Figure S2).

### Deletion of Platelet Cox-1 Suppresses Urinary Thromboxane Metabolite Excretion in Normolipidemic Mice (Ldlr$^{+/+}$) Fed a Standard Laboratory Diet After Tail Injury

Tail amputation activated platelet-dependent hemostasis. In Pf4-ΔCre mice, tail injury activated thromboxane (Tx) and $PGI_2$ biosynthesis in both sexes, as reflected by excretion of their urinary metabolites, 2,3-dinor TxB2 (TxM), and 2,3-dinor 6-keto $PGF_{1\alpha}$ (PGIM; Table 1). The increase in PGIM in male mice was not statistically significant compared with the baseline. Deletion of Cox-1 in platelets significantly suppresses TxM but not PGIM. PGDM (11,15-dioxo-9$_\alpha$-hydroxy-2,3,4,5-tetranorprostan-1,20-dioic acid), PGEM (7-hydroxy-5,11-diketotetranorprostane), and the $F_2$-isoprostane, 8,12-iso-iPF$_{2\alpha}$-VI were not significantly altered after tail injury in Pf4-ΔCre mice (Table S1). Similar trends were observed in Gp1ba-ΔCre mice of both sexes (Table 1; Table S1).

In summary, deletion of Cox-1 resulted in the expected and similar suppression of Tx in the setting of platelet activation in both lines. Due to differences in baseline urinary prostanoid metabolites, the percentage change with respect to baseline is also presented in Table 1.

### Deletion of Platelet Cox-1 Suppresses Prostanoids in Serum of Normolipidemic Mice

Platelets were activated ex vivo by exposing whole blood to a borosilicate glass tube for 1 hour at 37 °C. Deletion of Cox-1 in platelets in either line significantly suppresses serum levels of $TxB_2$, $PGD_2$, $PGE_2$, and $PGF_{2\alpha}$ in both sexes (Figure S3). As expected, given the absence of a vascular source, $PGI_2$ was below the limit of detection in serum.

### Deletion of Cox-1 in Platelets Increases Blood Loss in Ldlr$^{-/-}$ Mice

Mice fed an HFD for 12 weeks were used to measure the amount of blood loss after tail amputation to evaluate the hemostatic role of Cox-1 in activated platelets. Deletion of Cox-1 in platelets significantly increased blood loss in mice in both sexes (Figure 1A, 1B, 1E, and 1F) in both lines. Reflecting blood loss, hemoglobin levels were significantly higher in mice deficient in platelet Cox-1 (Figure 1C, 1D, 1G, and 1H).

### Platelet Cox-1 Promotes Thrombogenesis in Hyperlipidemic Mice (Ldlr$^{-/-}$) on a Standard Laboratory Diet

The time to vascular occlusion after a photochemical-induced carotid vascular injury in female mice was

**Table 1. Deletion of Platelet Cox-1 Suppresses Urinary Thromboxane Metabolite Excretion (TxM) in Normolipidemic Mice (Ldlr$^{+/+}$) After Tail Injury**

| | BL | | Tail injury | | BL | | Tail injury | |
|---|---|---|---|---|---|---|---|---|
| ng/mg creatinine | Controls | Platelet Cox-1$^{-/-}$ | Controls | Platelet Cox-1$^{-/-}$ | Controls | Platelet Cox-1$^{-/-}$ | Controls | Platelet Cox-1$^{-/-}$ |
| | Pf4-ΔCre female mice | | | | Pf4-ΔCre male mice | | | |
| TxM<br>%BL<br>*P* value*<br>*P* value† | 121±12 | 121±26<br>>0.99 | 201±32<br>176±31<br>0.011 | 98.7±18<br>89±10<br>0.013<br>0.99 | 56.8±7.5 | 32.5±4.6<br>0.055 | 80.9±8.8<br>153±17<br>0.00 | 28.5±4.1<br>93±17<br><0.001<br>>0.99 |
| PGIM<br>%BL<br>*P* value*<br>*P* value† | 2.27±0.2 | 2.57±0.4<br>>0.99 | 3.77±0.5<br>196±41<br>0.040 | 2.90±0.6<br>123±25<br>0.39<br>>0.99 | 2.88±0.2 | 2.40±0.1<br>>0.99 | 4.24±0.8<br>146±22<br>0.064 | 2.89±0.5<br>117±14<br>0.17<br>0.98 |
| | Gp1ba-ΔCre female mice | | | | Gp1ba-ΔCre male mice | | | |
| TxM<br>%BL<br>*P* value*<br>*P* value† | 30.7±2.2 | 24.2±2.9<br>0.19 | 42.3±3.0<br>140±8.6<br><0.001 | 17.1±2.5<br>74±8.4<br><0.001<br>0.021 | 16.7±3.0 | 13.3±1.7<br>0.96 | 29.5±7.3<br>182±22<br>0.010 | 13.2±1.5<br>118±20<br>0.003<br>>0.99 |
| PGIM<br>%BL<br>*P* value*<br>*P* value† | 0.78±0.0 | 0.88±0.2<br>>0.99 | 0.85±0.2<br>111±28<br>>0.99 | 0.86±0.2<br>110±28<br>>0.99<br>>0.99 | 0.81±0.1 | 0.74±0.1<br>>0.99 | 1.12±0.3<br>128±29<br>0.50 | 1.02±0.1<br>152±27<br>>0.99<br>0.37 |

Fasting (10 AM–5 PM) urine samples from mice on a standard laboratory diet were collected before and 2 days after tail injury, and prostanoids levels (PGIM, TxM, and M) were analyzed by liquid chromatography/mass spectrometry, as described in the Supplemental Methods. Due to differences in BL values between the 2 Cres, the changes after tail injury were expressed as %BL with respect to control or platelet Cox-1$^{-/-}$; (control at tail injury/control at BL)×100; and (platelet Cox-1$^{-/-}$ at tail injury/platelet Cox-1$^{-/-}$ at BL)×100. The 2-way ANOVA showed that urinary TxM and PGIM were significantly affected by tail injury, and deletion of Cox-1 affected TxM. The Bonferroni multiple comparison test was used to test for significant differences between groups (controls vs platelet Cox-1$^{-/-}$ mice) and treatments (BL vs tail injury). Data are expressed as means±SEMs. $P<0.05$ was considered significant. BL indicates baseline; Cox-1, cyclooxygenase-1; Gp1ba, glycoprotein 1bα; Ldlr, low-density lipoprotein receptor; M, metabolite; Pf4, platelet factor 4; PGIM, 2,3-dinor 6-keto $PGF_{1\alpha}$; and TxM, 2,3-dinor $TxB_2$.

*$P$ values between controls and platelet Cox-1$^{-/-}$ at BL or tail injury.

†$P$ values between BL and tail injury for controls or platelet Cox-1$^{-/-}$. Controls: Pf4-ΔCre (n=10 females and 10 males) or Gp1ba-ΔCre (n=9 females and 8 males), platelet Cox-1$^{-/-}$- Pf4-ΔCre/Cox-1$^{F/F}$ (n=7 females and 7 males), or Gp1ba-ΔCre/Cox-1$^{F/F}$ (n=8 females and 13 males).



significantly increased in both lines of Cox-1$^{-/-}$ mice compared with controls (Figure 2A).

For male mice, thrombosis was monitored using laser-induced injury of small arteries in the cremaster muscle in conjunction with intravital microscopy. Again, deletion of Cox-1 in platelets restrains thrombogenesis comparably in both lines (Figure 2B). Maximal thrombus size was significantly reduced in Cox-1$^{-/-}$ mice (Figure 2C).

## Contrasting Impact of Pf4-ΔCre–Mediated and Gp1ba-ΔCre–Mediated Deletion of Platelet Cox-1 on Atherogenesis in Hyperlipidemic Mice

Feeding Pf4-ΔCre mice an HFD for 12, 24, and 36 weeks significantly increased atherosclerotic plaque area relative to the total area, as assessed by en face lesion analysis (Figure 3A). Deletion of Cox-1 significantly increased lesional plaque accumulation at 36 weeks in female mice and at 24 and 36 weeks in male mice. By contrast, in Gp1ba-ΔCre mice, there were significant increases in atherosclerotic lesions with feeding time in mice regardless of genotype (Figure 3B; female and male), but deletion of Cox-1 significantly restrained lesional plaques at 36 weeks in female mice and at 24 and 36 weeks in male mice. Representative en face whole aortic lesion images stained with Sudan IV dye of male mice on 24 and 36 weeks of HFD are shown (Figure 3A and 3B, right).

Consistent with the en face analyses, aortic root lesion burden, as reflected by hematoxilin and eosin staining, was significantly increased in Cox-1–deficient Pf4Δ-Cre mice, while a reduction in aortic root lesion burden was observed in Cox-1$^{-/-}$–deficient Gp1ba-ΔCre mice (Figure 3C and 3D).

Mice from both lines fed an HFD gained body weight (Figure S4A and S4B). However, deletion of Cox-1 did not significantly alter weight, systolic blood pressure, heart rate, blood glucose, or triglycerides (Table S2) in either line or sex (Figures S4 and S5) fed an HFD.

## Deletion of Platelet Cox-1 Suppresses Urinary Prostanoid Metabolites in Hyperlipidemic Mice (Ldlr$^{-/-}$)

Urinary prostaglandin metabolites were measured in male mice after feeding an HFD for 24 weeks. HFD significantly increased urinary TxM, PGIM, and PGDM in both sexes in Pf4-ΔCre mice (Table 2), and deletion of Cox-1 in platelets significantly reduced these metabolites. Urinary PGEM and $F_2$-isoprostane, 8,12-iso-$iPF_{2\alpha}$-VI were not statistically altered after feeding an HFD regardless of sex or genotype of the mice (Table S3).

By contrast, in Gp1baΔ-Cre mice, the increase in PGDM did not attain significance after feeding an HFD, and deletion of Cox-1 in platelets did not significantly

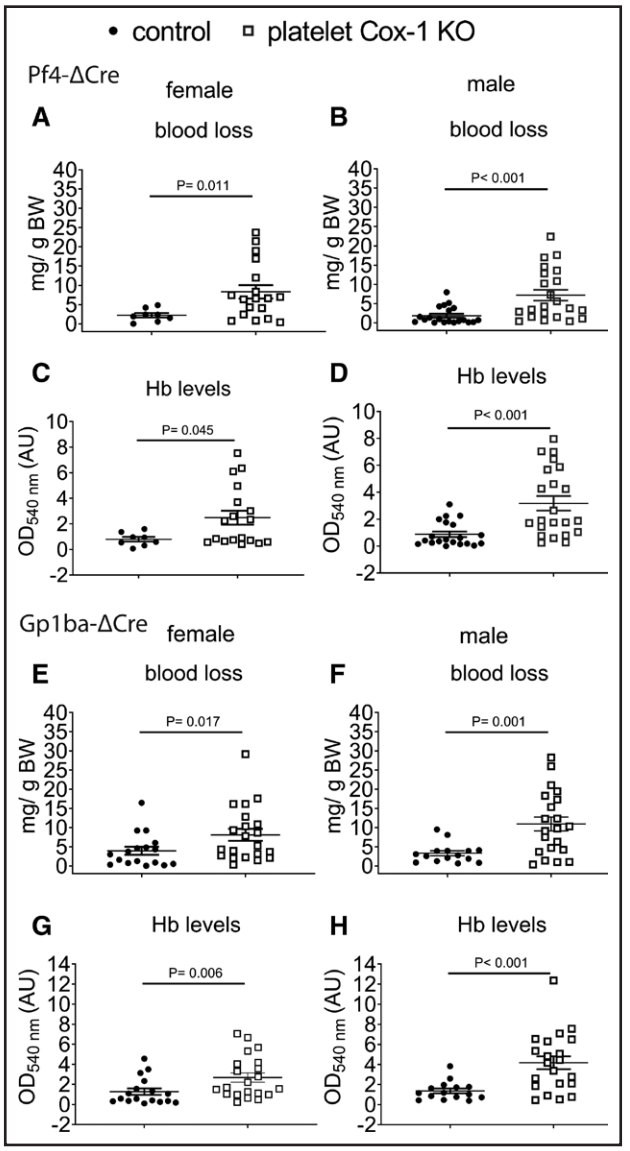


**Figure 1. Deletion of platelet Cox-1 (cyclooxygenase-1) increases blood loss in hyperlipidemic mice (Ldlr$^{-/-}$; low-density lipoprotein receptor) fed a high-fat diet (HFD).** Mice after 12 weeks on an HFD were used in this experiment; 2 mm of mouse tail was amputated under anesthesia, and blood was collected into a glass tube containing Drabkin reagent for 7.5 minutes (female) and 15 minutes (male). Pf4 (platelet factor 4)-ΔCre–mediated or Gp1ba (glycoprotein 1bα)-ΔCre–mediated deletion of Cox-1 in platelets significantly increased blood loss (Pf4-ΔCre: [**A**] female and [**B**] male; Gp1ba-ΔCre: [**E**] female and [**F**] male). Hemoglobin levels were significantly increased in platelet Cox-1$^{-/-}$ mice (Pf4-ΔCre: [**C**] female and [**D**] male; Gp1ba-ΔCre: [**G**] female and [**H**] male). Data are expressed as means±SEMs (Mann-Whitney *U* test, 1-tailed, n=8–21 per group for female mice, and n=15–22 per group for male mice). Controls: Pf4-ΔCre/Ldlr$^{-/-}$ or Gp1ba-ΔCre/Ldlr$^{-/-}$, platelet Cox-1 KO-Pf4-ΔCre/Cox-1$^{F/F}$/Ldlr$^{-/-}$, or Gp1ba-ΔCre/Cox-1$^{F/F}$/Ldlr$^{-/-}$. AU indicates absorbance units; BW, body weight; OD, optical density; and KO, knock-out.

suppress urinary PGIM. Urinary PGEM was significantly reduced in males after feeding an HFD regardless of genotype (Table 2; Table S3).

## Differential Impact on Lipopolysaccharide-Evoked Vascular Capacity to Form Prostanoids in Ldlr$^{-/-}$ Mice

We isolated whole aortas from mice fed an HFD and treated the aortas in cell culture media with lipopolysaccharide for 8 hours at 37 °C. Tx was suppressed in both Cox-1–deficient lines, perhaps reflecting residual platelet contamination. However, $PGE_2$ and $PGD_2$ were only suppressed in the Cox-1–depleted Pf4-ΔCre line (Table S4).

In summary, while Tx biosynthesis (urinary TxM) and the aortic capacity to generate Tx after lipopolysaccharide treatment are suppressed in both lines, the formation of prostanoids that can mediate an anti-inflammatory effect on atherogenesis was depressed in vivo (PGIM) and ex vivo (lipopolysaccharide-evoked $PGE_2$ and $PGD_2$) only in the Cox-1–depleted Pf4-ΔCre line.

## Differential Impact in Cox-1 Gene Expression in Aortas and Peritoneal Cells of Male Ldlr$^{-/-}$ Mice Fed an HFD for 24 Weeks

Aortic Cox-1 mRNA was reduced to a greater extent in Pf4-ΔCre Cox-1$^{-/-}$ mice (≈76%) than in Gp1ba-ΔCre male mice (≈49%) after feeding an HFD for 24 weeks (Figure S6A). Cox-1 expression was also reduced in peritoneal cells of this line but not in the Gp1ba-ΔCre mice (Figure S6B). Pf4-ΔCre Cox-2 mRNA was not altered by Cox-1 depletion (Figure S6A and S6B).

## scRNA-seq of Mouse Aortas

In an exploratory study to investigate the divergent atherosclerotic phenotypes between the 2 approaches to deletion of Cox-1 in Ldlr$^{-/-}$ mice, we performed scRNA sequencing using aortas from male mice fed an HFD for 24 weeks.

scRNA-seq analyses revealed 9 distinct cell clusters with unique marker genes as displayed in Uniform Manifold Approximation and Projections. As shown in Figure 4A, one of the main differences between the 2 mouse lines was the identification of a cell cluster (black rectangle) that displayed signature genes of stem cells, endothelial cells, and monocytes.[25–27] Mouse aortas from the Pf4-ΔCre mice (both control and platelet Cox-1 knock-outs) had many more stem cells, endothelial cells, and monocytes than those from the Gp1ba-ΔCre mice irrespective of Cox-1 expression. We studied vascular smooth muscle cells in more detail because they constituted about 50% of the isolated cells from the atherosclerotic aortas. Additionally, the phenotypic switching of smooth muscle cells during atherogenesis has been related to the pathophysiology of this disease.[25,28] KEGG (Kyoto Encyclopedia of Genes and Genomes) pathway

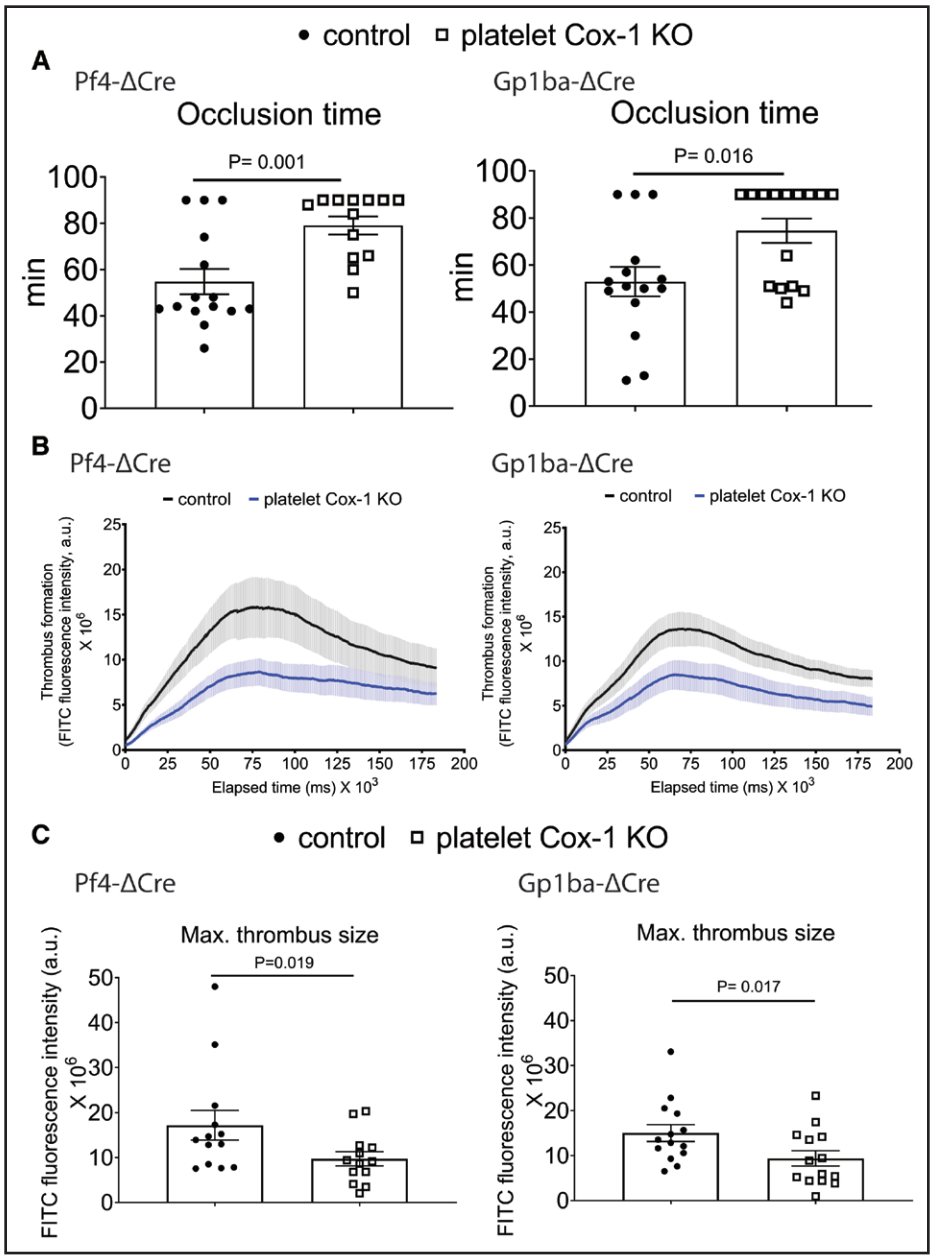


**Figure 2. Platelet Cox-1 (cyclooxygenase-1) promotes thrombogenesis in Ldlr$^{-/-}$ (low-density lipoprotein receptor) mice of both sexes.**

The 12- to 14-week-old female and male Ldlr$^{-/-}$ mice on a standard laboratory diet were used in these experiments. The time to thrombotic carotid artery occlusion after photochemical injury was extended in female platelet Cox-1$^{-/-}$ hyperlipidemic mice ([**A**] Pf4 [platelet factor 4]-ΔCre [**left**] and Gp1ba [glycoprotein 1bα]-ΔCre [**right**]). A Mann-Whitney *U* test (1-tailed) revealed a significant effect of genotype on occlusion time. Data are expressed as means±SEMs. n=13 to 15 per group. **B**, Thrombogenesis in cremaster arterioles after laser-induced injury in male platelet Cox-1$^{-/-}$ hyperlipidemic mice. Thrombus formation was visualized in real time with fluorescently labeled platelets, as described in the Supplemental Methods. Median-integrated fluorescence intensity of platelets representing thrombus formation was plotted vs time after laser-induced injury of the cremaster arteriole vessel wall. Fluorescence intensity from 10 thrombi was averaged from each mouse. Data corresponding to maximal thrombus size were extracted from the fluorescence-time curves and averaged ([**C**] Pf4-ΔCre [**left**] and Gp1ba-ΔCre [**right**]). A Mann-Whitney *U* test (1-tailed) revealed a significant effect of Cox-1 deletion on maximal thrombus formation. Data are expressed as means±SEMs. n=13 to 14 per group. Controls: Pf4-ΔCre/Ldlr$^{-/-}$ or Gp1ba-ΔCre/Ldlr$^{-/-}$, platelet Cox-1 KO-Pf4-ΔCre/Cox-1$^{F/F}$/Ldlr$^{-/-}$, or Gp1ba-ΔCre/Cox-1$^{F/F}$/Ldlr$^{-/-}$. FITC indicates fluorescein isothyiocyanate; and KO, knock-out.

analyses associated with changes in gene expression showed that the TCA (citric acid cycle), carbon metabolism, spliceosome, and protein processing in the ER genes were differentially altered between the 2 lines (Figure 4E). For macrophages, pathway enrichment analyses revealed that glycosphingolipid signaling was differentially expressed and modulated by Cox-1 deletion in the 2 lines (Figure S7A). Differential gene expression

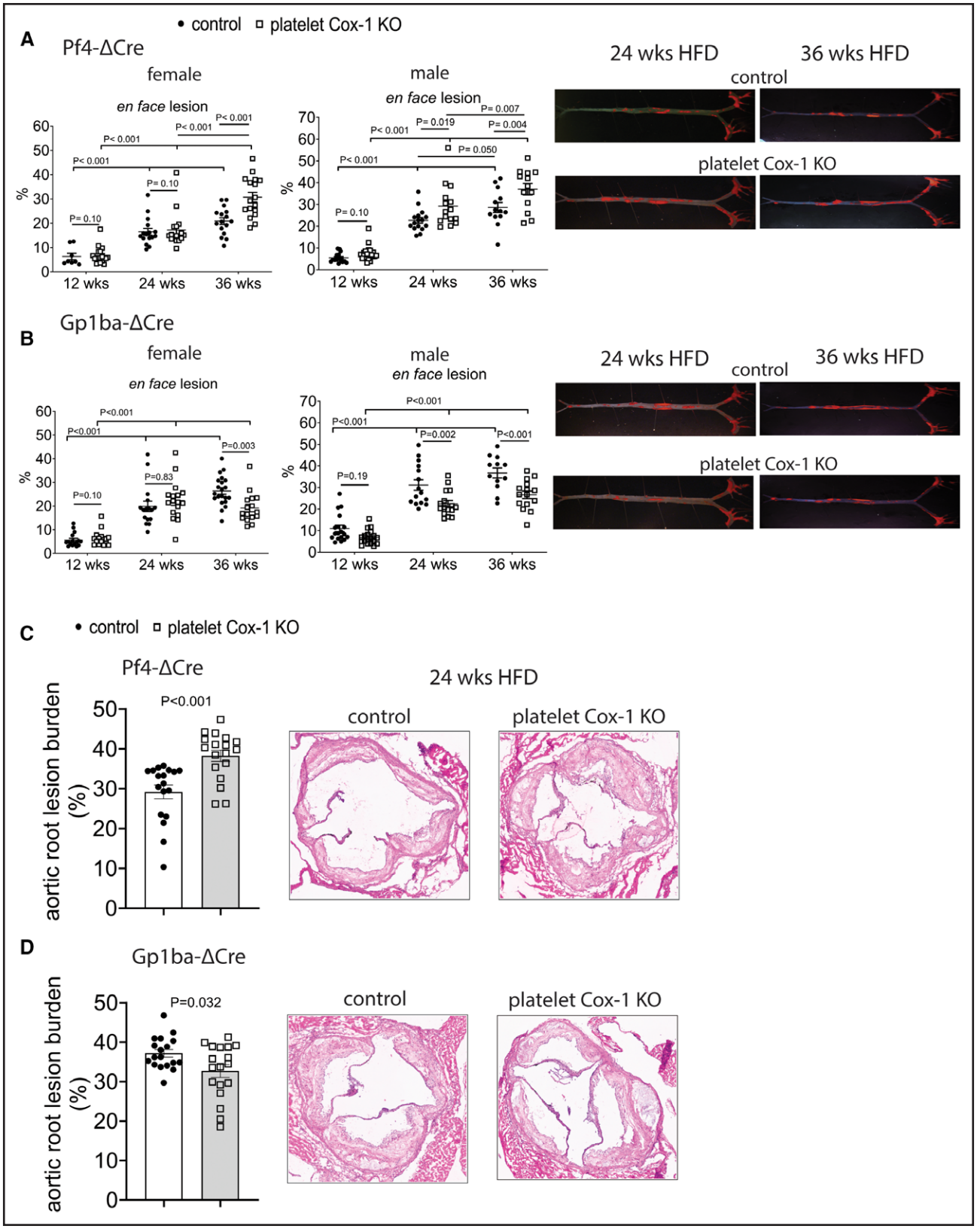


**Figure 3. Pf4 (platelet factor 4)-ΔCre–mediated deletion of platelet Cox-1 (cyclooxygenase-1) promotes atherogenesis in Ldlr$^{-/-}$ (low-density lipoprotein receptor) mice, while Gp1ba (glycoprotein 1bα)-ΔCre–mediated deletion restrains atherogenesis.** Aortic atherosclerotic lesion burden, represented by the percentage of lesion area stained with Sudan VI to total aortic area, was quantified by en face analysis of aortas from mice fed a high-fat diet (HFD) for 12, 24, and 36 weeks. **A**, Lesion area increased with feeding time, and Pf4-ΔCre–mediated deletion of Cox-1 increased lesion burden in mice of both sexes. **B**, However, Gp1ba-ΔCre–mediated Cox-1 (*Continued*)

analyses of smooth muscle cells; macrophages; and stem cells, endothelial cells, and monocytes revealed upregulation of several genes associated with anti-inflammatory signaling in Gp1ba-ΔCre–mediated deletion of Cox-1 in platelets (Figure 4F; Figure S7B–S7D). Despite Bpifa1 (bacterial permeability family member A1) being differentially expressed in T cells, relevant KEGG pathways (focal adhesion, oxidative phosphorylation, and protein processing in ER) were equally impacted between controls and platelet Cox-1$^{-/-}$ mice of both Cres (Figure S7E). Pf4 expression was restricted to macrophages but was unaltered by Cre or genotype (Figure S7F). Cell-type proportions are presented in Figure S7G.

## Cox-1, Cox-2, Pf4, and Tnf-α mRNA Levels of Aortic CD3$^+$ T and CD11b$^+$ Cells

We isolated immune cells from mouse aortas by fluorescence-activated cell sorting to perform rt-qPCR. In CD3$^+$ T cells, Cox-1 mRNA levels were significantly reduced in platelet Cox-1$^{-/-}$ mice mediated by Pf4-ΔCre but not in Gp1ba-ΔCre mice (Figure S8A). Interestingly, Pf4 was detected only in CD3$^+$ T cells from Pf4-ΔCre mice and was significantly decreased in platelet Cox-1$^{-/-}$ CD3$^+$ T cells. However, no significant differences in Cox-1 mRNA levels were detected in CD11b$^+$ cells between control and platelet Cox-1$^{-/-}$ mice of both Cres. Cox-2 mRNA levels in CD3$^+$ T cells were significantly reduced in Pf4-ΔCre Cox-1$^{-/-}$ mice, but in CD11b$^+$ cells, Cox-2 levels increased in Pf4-ΔCre Cox-1$^{-/-}$ mice and decreased in Gp1ba-ΔCre mice. We tried to characterize CD11b$^+$ cells based on the M1 or M2 macrophage markers[29] and M1 (Tnf-α [tumor necrosis factor] and IL-17a [interleukin]) or M2 (IL-4 and IL-13) by rt-qPCR. Unexpectedly, only Tnf-α was significantly elevated in CD11b$^+$ cells from Pf4-ΔCre Cox-1$^{-/-}$ mice (Figure S8B). IL-17A, IL-4, and IL-13 levels were below the limit of detection. The gating strategy for sorting immune cells from mouse aortas is presented in Figure S8C.

## Inflammasome Signaling Pathway Is Activated in Pf4-ΔCre Male Ldlr$^{-/-}$ Mice

Consistent with the scRNA-seq results, Pf4-ΔCre–mediated deletion of Cox-1 in platelets significantly increased plasma levels of IL-β compared with controls after 12 weeks on an HFD (Figure S9A). No significant differences were observed in Gp1ba-ΔCre mice (Figure S9B). Splenic cleaved-caspase-1 protein expression was significantly upregulated only in platelet Cox-1$^{-/-}$ Pf4-ΔCre mice (Figure S9C). Administration of an inflammasome inhibitor (MCC950) abrogated the differences in atherosclerotic plaque lesions, cleaved-caspase-1 protein, and plasma IL-1β levels between controls and these platelet Cox-1$^{-/-}$ mice (Figure S9E).

## Pf4-ΔCre–Mediated Deletion of Cox-1 in Platelets Decreases Reverse Cholesterol Transport in Male Ldlr$^{-/-}$ Mice

Plasma levels of HDL-C (high-density lipoprotein receptor-cholesterol) were significantly decreased in platelet Cox-1$^{-/-}$ mice mediated by Pf4-ΔCre after feeding an HFD for 24 weeks (Table S2). These findings prompted us further to investigate reverse cholesterol transport. Abc (ATP-binding cassette)a1 and Abcg1 mRNA expression levels were downregulated in platelet Cox-1$^{-/-}$ mice compared with controls (Figure S10A). Consistent with these results, liver H$^3$-cholesterol levels were significantly decreased in platelet Cox-1$^{-/-}$ mice compared with controls (Figure S10B). No significant differences in H$^3$-cholesterol levels were detected in the plasma and feces between controls and platelet Cox-1$^{-/-}$ mice (Figure S10B).

## Gp1ba-ΔCre–Mediated Deletion of Cox-1 in Platelets Reduces Biomarkers of Inflammation in Male Ldlr$^{-/-}$ Mice

Plasma levels of HDL-C were significantly increased in male platelet Cox-1$^{-/-}$ mice mediated by Gp1ba-ΔCre after feeding an HFD for 12 weeks (Table S2), and plasma levels of MIP-1α (macrophage inflammatory protein-1α) and MCP-1 (monocyte chemoattractant protein 1) were significantly decreased (Figure S11A and S11B).

Deletion of platelet Cox-1 in either line did not significantly alter plasma levels of IL-10 and IL-13 in mice fed an HFD for 24 weeks (Figure S11C and S11D).

Orthogonal partial least-squares discriminant analysis revealed a distinct separation of plasma metabolites between Gp1ba-ΔCre controls (red) and platelet Cox-1$^{-/-}$ (green) mice ($P$=0.02; Q2=0.52; Figure S12A).

**Figure 3 Continued.** deletion in platelets restrained lesion burden. For (**A** and **B**), a 2-way ANOVA showed that en face aortic lesion burden was significantly affected by feeding time or deletion of Cox-1 in platelets. The Bonferroni multiple comparison test was used to test for significant differences between controls and platelets Cox-1$^{-/-}$ mice or feeding time. Data are expressed as means±SEMs. *$P$<0.05; n=8 to 24 per group. En face aortic images of male hyperlipidemic mice on an HFD diet for 24 and 36 weeks ([**A**] Pf4-ΔCre and [**B**] Gp1ba-ΔCre). **C** and **D**, Aortic root lesion burden was quantified by hematoxilin and eosin staining of cross-sections from male mice fed an HFD for 24 weeks. The area of aortic root lesions was expressed as a percentage of the total area of the vessel minus the luminal area. Representative cross-sectional images are shown (**right**). Pf4-ΔCre–mediated deletion of Cox-1 increased lesion burden in male mice (**C**), while Gp1ba-ΔCre reduced it (**D**). For (**C** and **D**), a Mann-Whitney *U* test (1-tailed) revealed a significant effect of Cox-1 deletion in platelets on aortic root lesion burden progression. Data are expressed as means±SEMs. n=8 to 9 per group. Controls: Pf4-ΔCre/Ldlr$^{-/-}$ or Gp1ba-ΔCre/Ldlr$^{-/-}$, platelet Cox-1 KO-Pf4-ΔCre/Cox-1$^{F/F}$/Ldlr$^{-/-}$, or Gp1ba-ΔCre/Cox-1$^{F/F}$/Ldlr$^{-/-}$. KO indicates knock-out.

**Table 2. Deletion of Platelet Cox-1 Suppresses Urinary Prostanoid Metabolites in Hyperlipidemic Mice (Ldlr$^{-/-}$) Fed an HFD**

| | BL | | 24-wk HFD | | BL | | 24-wk HFD | |
|---|---|---|---|---|---|---|---|---|
| ng/mg creatinine | Controls | Platelet Cox-1$^{-/-}$ | Controls | Platelet Cox-1$^{-/-}$ | Controls | Platelet Cox-1$^{-/-}$ | Controls | Platelet Cox-1$^{-/-}$ |
| | Pf4-ΔCre female mice | | | | Pf4-ΔCre male mice | | | |
| TxM<br>*P* value*<br>*P* value† | 173±15 | 82.4±6.6<br>0.19 | 733±71<br><0.001 | 207±26<br><0.001<br>0.046 | 131±27 | 31.8±3.8<br>0.12 | 543±68<br><0.001 | 99.2±13<br><0.001<br>0.32 |
| %BL | | | 487±72 | 251±32 | | | 541±83 | 362±65 |
| PGIM<br>*P* value*<br>*P* value† | 3.30±0.3 | 3.36±0.3<br>>0.99 | 6.20±0.4<br><0.001 | 3.60±0.3<br><0.001<br>>0.99 | 6.29±1.5 | 5.60±1.4<br>>0.99 | 31.8±3.8<br><0.001 | 20.5±2.3<br>0.006<br><0.001 |
| %BL | | | 237±47 | 114±11 | | | 646±82 | 521±77 |
| PGDM<br>*P* value*<br>*P* value† | 32.7±5.3 | 18.0±1.5<br>0.006 | 38.7±3.3<br>0.34 | 16.2±2.2<br><0.001<br>>0.99 | 83.3±20 | 30.4±3.9<br>0.005 | 116±11<br>0.034 | 36.7±4.8<br><0.001<br>>0.99 |
| %BL | | | 155±23 | 103±17 | | | 187±21 | 145±26 |
| | Gp1ba-ΔCre female mice | | | | Gp1ba-ΔCre male mice | | | |
| TxM<br>*P* value*<br>*P* value† | 83.2±5.1 | 46.2±4.6<br>0.23 | 305±34<br><0.001 | 105±12<br><0.001<br>0.030 | 32.9±7.7 | 21.5±3.3<br>0.75 | 105±15<br><0.001 | 38.4±6.6<br><0.001<br>0.39 |
| %BL | | | 370±32 | 245±27 | | | 508±124 | 226±47 |
| PGIM<br>*P* value*<br>*P* value† | 1.92±0.1 | 1.45±0.1<br>0.23 | 2.79±0.3<br>0.005 | 2.25±0.2<br>0.16<br>0.008 | 2.52±0.6 | 1.96±0.2<br>>0.99 | 9.93±1.1<br><0.001 | 7.98±0.6<br>0.10<br><0.001 |
| %BL | | | 148±14 | 179±27 | | | 459±49 | 455±53 |
| PGDM<br>*P* value*<br>*P* value† | 14.0±0.9 | 14.3±1.0<br>>0.99 | 17.3±1.5<br>0.043 | 10.0±0.9<br><0.001<br>0.006 | 30.9±6.2 | 20.7±1.9<br>0.13 | 36.1±3.5<br>0.65 | 25.7±2.8<br>0.12<br>0.65 |
| %BL | | | 129±12 | 74±7 | | | 175±38 | 141±19 |

Fasting (10 AM–5 PM) urine samples from mice were collected before and after 24 wk on an HFD, and prostanoid metabolites (PGIM, TxM, tetranor PGDM, and M) were analyzed by liquid chromatography/mass spectrometry, as described in the Supplemental Methods. Due to differences in baseline values between the 2 Cres, the changes after 24 wk of HFD were expressed as %BL; (control at 24-wk HFD/control at baseline)×100; and (platelet Cox-1$^{-/-}$ at 24-wk HFD/platelet Cox-1$^{-/-}$ at baseline)×100. A 2-way ANOVA showed that TxM, PGIM, and PGDM were significantly affected by Cox-1 deletion or 24 wk of HFD. The Bonferroni multiple comparison test was used to test for significant differences between groups (controls vs platelet Cox-1$^{-/-}$) and treatments (baseline vs 24-wk HFD). BL indicates baseline; Cox-1, cyclooxygenase-1; Gp1ba, glycoprotein 1bα; HFD, high-fat diet; Ldlr, low-density lipoprotein receptor; M, metabolite; Pf4, platelet factor 4; PGDM, 11,15-dioxo-9$_{\alpha}$-hydroxy-2,3,4,5-tetranorprostan-1,20-dioic acid; and PGIM, 2,3-dinor 6-keto PGF$_{1\alpha}$.

*$P$ values between controls and platelet Cox-1$^{-/-}$ at baseline or 24-wk HFD.

†$P$ values between baseline and 24-wk HFD for controls or platelet Cox-1$^{-/-}$. Data are expressed as means±SEMs; n=15–16 per group. $P$<0.05 was considered significant. Controls: Pf4-ΔCre/Ldlr$^{-/-}$ or Gp1ba-ΔCre/Ldlr$^{-/-}$, platelet Cox-1$^{-/-}$-Pf4-ΔCre/Cox-1$^{F/F}$/Ldlr$^{-/-}$, or Gp1ba-ΔCre/Cox-1$^{F/F}$/Ldlr$^{-/-}$.

No such separation was observed between Pf4-ΔCre$^{+/KI}$ controls (blue) and platelet Cox-1$^{-/-}$ (purple) mice ($P$>0.1; Q2=0). MetaboAnalyst pathway analysis revealed amino acid metabolic pathways were impacted in Gp1ba-ΔCre–mediated deletion of Cox-1 in platelets, especially glycine, serine, threonine, tyrosine, alanine, aspartate, and glutamate metabolism (Figure S12B). Indeed, plasma levels of α-tocopherol were significantly increased in Gp1ba-ΔCre platelet Cox-1$^{-/-}$ mice compared with controls (Figure S12C).

Products of the lipoxygenase and epoxygenase pathways of AA metabolism were unaltered by platelet Cox-1 deletion in either line (data not shown).

## DISCUSSION

Genetic ablation of platelet Cox-1 in mice would be expected to recapitulate the effects of low-dose aspirin—suppression of Tx and PGD formation, impairment of hemostasis, and restraint of thrombogenesis and atherogenesis.[30–32]

There are 2 major findings in this article. First, under the conditions of no insult or acute injury with short-term stress, the use of Pf4-ΔCre or Gp1ba-ΔCre to effect deletion of Cox-1 in platelets resulted in comparable and expected suppression of ex vivo platelet aggregation, prostanoid formation, impairment of hemostasis, and restraint of thrombogenesis.[9,17,31,33] This was an important comparison given concerns about the relative efficiency of recombination, the potential impact on platelet-dependent thrombogenesis of partial loss of Gp1ba, and the use of flox/flox but not Cre-positive controls. As expected, urinary lipoxygenase and epoxygenase products of AA were unaltered by Cox-1 deletion in either line. The increase in $PGI_2$ biosynthesis coincident with Tx after tail injury is expected, reflecting the interaction of platelets with vascular endothelial cells, which produce $PGI_2$ to counteract the vasoconstrictive and

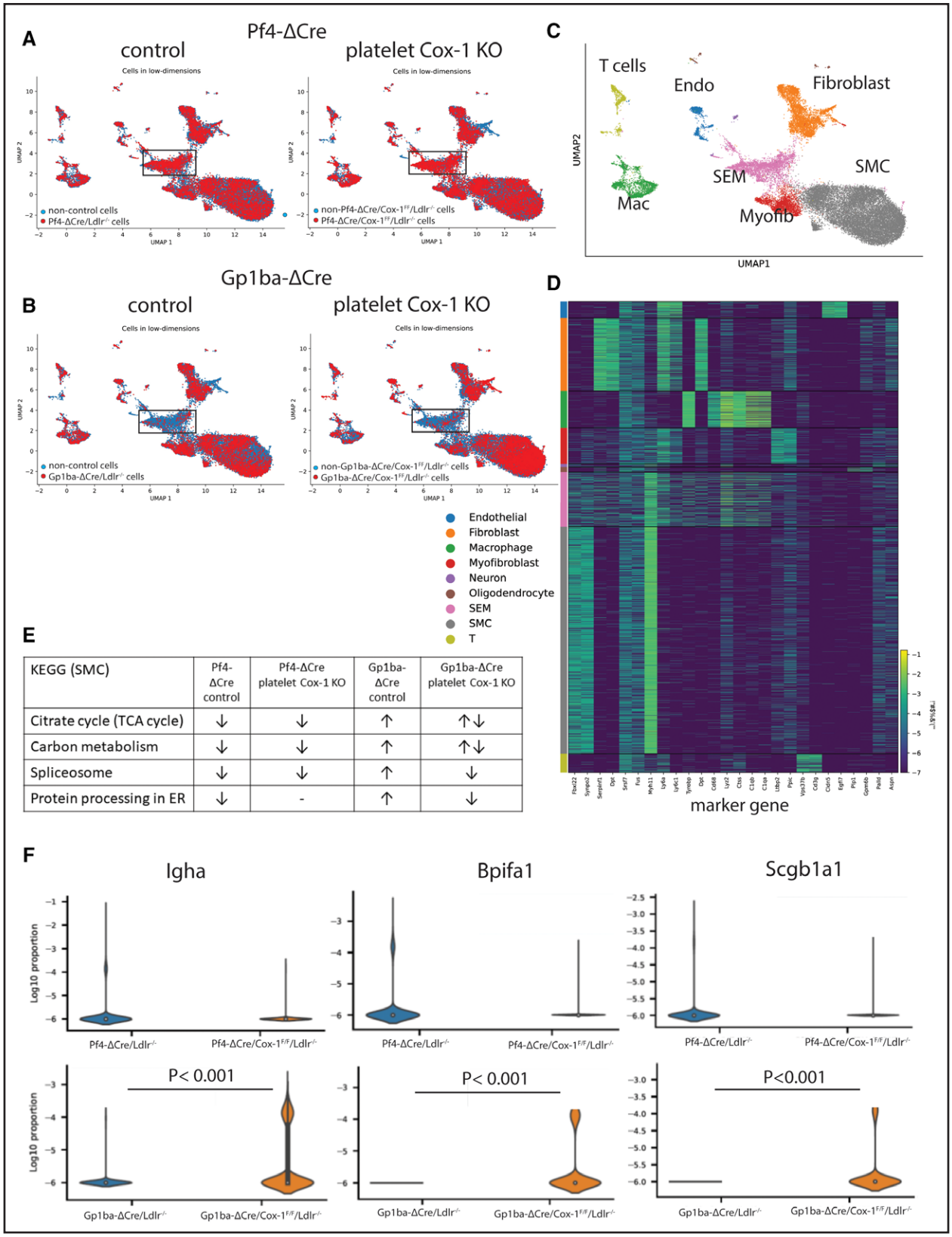


| KEGG (SMC) | Pf4-ΔCre control | Pf4-ΔCre platelet Cox-1 KO | Gp1ba-ΔCre control | Gp1ba-ΔCre platelet Cox-1 KO |
|---|---|---|---|---|
| Citrate cycle (TCA cycle) | ↓ | ↓ | ↑ | ↑↓ |
| Carbon metabolism | ↓ | ↓ | ↑ | ↑↓ |
| Spliceosome | ↓ | ↓ | ↑ | ↓ |
| Protein processing in ER | ↓ | - | ↑ | ↓ |

**Figure 4. Single-cell RNA sequencing analysis of mouse aorta revealed the presence of stem cells, endothelial cells, and monocytes (SEM) in higher abundance in Pf4 (platelet factor 4)-ΔCre male Ldlr$^{-/-}$ (low-density lipoprotein receptor) mice fed a high-fat diet (HFD) for 24 weeks.**

Uniform Manifold Approximation and Projection (UMAP) representation of aligned gene expression data of mouse atherosclerotic aorta from Pf4-ΔCre (**A**) or Gp1ba (glycoprotein 1bα)-ΔCre (**B**) mice fed an HFD for 24 weeks. Inflammatory SEM cells (in black rectangle) were present in a larger quantity in Pf4-ΔCre mice compared with Gp1ba-ΔCre mice regardless of the deletion of Cox-1 (cyclooxygenase-1) (*Continued*)

platelets aggregation effects of Cox-1-derived thromboxane $A_2$.[32,34] Interestingly, Cox-1 depletion reduced this protective PGI2 response only in the Pf4-ΔCre line. While Cox-1 deletion suppressed urinary TxM when an increase was evoked by either tail injury or an HFD, the failure to detect an impact on basal TxM likely reflected a deficiency of power relative to the low levels of the metabolite in mice. Low-dose aspirin markedly suppressed urinary TxM in humans.[35] When whole blood was activated ex vivo, all serum prostanoids were fully suppressed by the deletion of Cox-1 in platelets driven by either Pf4-ΔCre or Gp1ba-ΔCre recombination. In this assay, there is no vascular source of $PGI_2$, and suppression of platelet Tx (and $PGD_2$) formation would be expected to reduce platelet-dependent leukocyte activation and consequently $PGE_2$. It is worth noting that differences in baseline prostanoid metabolites between the 2 models may reflect any number of things including leakiness of Cre-mediated recombination.

The second major observation was a surprise. While Gp1ba-ΔCre–targeted deletion of platelet Cox-1 restrained atherogenesis in hyperlipidemic mice as expected, Pf4-ΔCre–mediated deletion of Cox-1 had the opposite effect. While an off-target extra-platelet effect was unexpected, the differential impacts on aortic Cox-1 mRNA levels and urinary PGIM could have contributed to atherogenesis in the Pf4-ΔCre mice. Deletion of its receptor—the IPr (I prostanoid receptor)—accelerates atherogenesis in hyperlipidemic mice.[36] Furthermore, Pf4 was extant only in macrophages in our scRNA analysis. The capacity for lipopolysaccharide-evoked Tx formation by the atherosclerotic vasculature was reduced by Cox-1 depletion in both lines; however, there was a concomitant depletion of $PGE_2$ and $PGD_2$, both of which have anti-inflammatory properties[37] only in the Pf4-ΔCre line. Thus, a contrasting impact on atheroprotective prostaglandin formation—reactive $PGI_2$ by the vasculature and $PGE_2$ and $PGD_2$—likely by infiltrating macrophages may have contributed to the divergent impact of Cox-1 depletion on atherogenesis in the 2 lines.

To address this further, we sought differences in gene expression, inflammatory, and lipid biomarkers and in the plasma metabolome between the 2 lines.

Consistent with restraint of atherogenesis and suppression of inflammatory soluble intracellular adhesion molecule-1 and MCP-1 in hyperlipidemic mice treated with low-dose aspirin,[38] aortic scRNA-seq analyses revealed that smooth muscle cells; macrophages; stem cells, endothelial cells, and monocytes; and T cells in the Gp1ba-ΔCre platelet Cox-$1^{-/-}$ mice expressed higher levels of genes associated with anti-inflammatory properties, including immunoglobulin (Igha [immunoglobulin heavy chain a] and Igkc), secretoglobin (Scgb1a1 [secretoglobin family 1A member 1], Scgb3a1 [secretoglobin family 3A member 1], and Scgb3a2 [secretoglobin family 3A member 2]), and Bpifa1. Administration of immunoglobulin to mice and genetic deletion of the latter genes modulate immune responses and activate inflammatory pathways in animal models.[39–41] In addition, the systemic inflammatory markers, MIP-1α and MCP-1, were reduced in the Gp1ba-ΔCre Cox-$1^{-/-}$ mice coincident with an increase in plasma levels of α-tocopherol and HDL-C.[42,43] In contrast, Pf4-ΔCre Cox-$1^{-/-}$ mice had lower anti-inflammatory gene expression and elevated plasma levels of IL-1β due to the activation of the inflammasome. Consistent with an inflammatory environment, $CD11b^+$ cells isolated from the atherosclerotic plaques of Pf4-ΔCre Cox-$1^{-/-}$ mice displayed M1-like macrophage markers. Plasma HDL-C and the capacity for reverse cholesterol transport were both reduced in Pf4-ΔCre platelet Cox-$1^{-/-}$ mice.

The expression of prostaglandin-related genes was mostly below the limit of detection in all the cell clusters identified in the scRNA analysis of the aorta. Despite this, Cox-1 mRNA in mouse aortas and peritoneal cells (50%–60% B cells, ≈30% macrophages, and 5%–10% T cells)[44] from mice fed an HFD, as well as $CD3^+$ T cells isolated from aortic plaques, as determined by rt-qPCR were markedly reduced in Pf4-ΔCre–mediated recombination compared with the deletion by Gp1ba-ΔCre.

Overall, we have evaluated the impact of Cox-1 deletion in platelets mediated by Pf4-ΔCre or Gp1ba-ΔCre on prostanoid biosynthesis and models of cardiovascular disease (Figure S13). Our data support the notion that despite potentially different impacts on platelet function, both models simulate the effects of low-dose aspirin on thrombosis, but they display a differential impact on atheroprotective prostanoids and inflammation, resulting in a divergent impact on atherogenesis.

**Figure 4 Continued.** in platelets. Red cells: cells that are the genotype of interest; blue cells: cells that are representative of all background transcripts. **C**, UMAP showing the distribution and identification of the 9 different cell clusters from the mouse aorta. **D**, Heatmap of the marker genes in each cluster selected as unique genes used for identification of each cluster. **E**, KEGG (Kyoto Encyclopedia of Genes and Genomes) pathway analysis of differentially expressed genes in smooth muscle cells (SMCs) revealed alteration in pathways associated with the TCA (citric acid cycle), carbon metabolism, spliceosome, and protein processing in ER signaling. **E**, Violin plots of the top differentially expressed genes associated with anti-inflammation showing upregulation in Gp1ba-ΔCre–mediated deletion of Cox-1 in platelets. **Top**, Pf4-ΔCre. **Bottom**, Gp1ba-ΔCre. Blue violin plots: controls; orange violin plots: platelet Cox-1 knockouts. A Mann-Whitney *U* test revealed a significant effect of Cox-1 deletion in platelets mediated by Gp1ba-ΔCre; $P<0.05$ was considered significant. Controls: Pf4-ΔCre/$Ldlr^{-/-}$ or ΔGp1ba-Cre/$Ldlr^{-/-}$, platelet Cox-1 KO-Pf4-ΔCre/Cox-$1^{F/F}$/$Ldlr^{-/-}$, or ΔGp1ba-Cre/Cox-$1^{F/F}$/$Ldlr^{-/-}$. ↑ indicates upregulation; ↓, downregulation; Bpifa1, bacterial permeability family member A1; ER, endoplasmic reticulum; Igha, immunoglobulin heavy chain a; KO, knock-out; and Scgb1a1, secretoglobin family 1A member 1.

## ARTICLE INFORMATION

Received October 26, 2023; accepted April 12, 2024.

### Affiliations

Institute for Translational Medicine and Therapeutics, Perelman School of Medicine (S.Y.T., R.L., H.M., B.J.A., E.J.H., A.S., U.S.D., R.J., R.M., G.R.G., E.R., T.G., A.M.W., G.A.F.), Department of Systems Pharmacology and Translational Therapeutics (O.A.M.-C., E.R., V.R.M., A.M.W.), Department of Genetics (G.R.G., G.A.F.), and Department of Medicine, Perelman School of Medicine (T.G., G.A.F.), University of Pennsylvania, Philadelphia. Now with Department of Translational Pharmacology, Bielefeld University, Germany (T.G.).

### Acknowledgments

The authors thank members of the Flow Cytometry Core at Children's Hospital of Philadelphia for assisting with fluorescence-activated cell sorting.

### Sources of Funding

This work was supported by NIH (grant HL062250).

### Disclosures

G.A. FitzGerald is the McNeil Professor of translational medicine and therapeutics and held a Merit Award from the American Heart Association during the performance of this work. The other authors report no conflicts.

### Supplemental Material

Supplemental Methods
Figures S1–S13
Tables S1–S3
Major Resources Table

## REFERENCES

1. Ricciotti E, FitzGerald GA. Aspirin in the prevention of cardiovascular disease and cancer. *Annu Rev Med*. 2021;72:473–495. doi: 10.1146/annurev-med-051019-102940
2. Patrono C, Baigent C. Role of aspirin in primary prevention of cardiovascular disease. *Nat Rev Cardiol*. 2019;16:675–686. doi: 10.1038/s41569-019-0225-y
3. Bowman L, Mafham M, Wallendszus K, Stevens W, Buck G, Barton J, Murphy K, Aung T, Haynes R, Cox J, et al; ASCEND Study Collaborative Group. Effects of aspirin for primary prevention in persons with diabetes mellitus. *N Engl J Med*. 2018;379:1529–1539. doi: 10.1056/NEJMoa1804988
4. Hybiak J, Broniarek I, Kiryczynski G, Los LD, Rosik J, Machaj F, Slawinski H, Jankowska K, Urasinska E. Aspirin and its pleiotropic application. *Eur J Pharmacol*. 2020;866:172762. doi: 10.1016/j.ejphar.2019.172762
5. Pietrocola F, Castoldi F, Markaki M, Lachkar S, Chen G, Enot DP, Durand S, Bossut N, Tong M, Malik SA, et al. Aspirin recapitulates features of caloric restriction. *Cell Rep*. 2018;22:2395–2407. doi: 10.1016/j.celrep.2018.02.024
6. Nagy Z, Vogtle T, Geer MJ, Mori J, Heising S, Di Nunzio G, Gareus R, Tarakhovsky A, Weiss A, Neel BG, et al. The Gp1ba-Cre transgenic mouse: a new model to delineate platelet and leukocyte functions. *Blood*. 2019;133:331–343. doi: 10.1182/blood-2018-09-877787
7. Pertuy F, Aguilar A, Strassel C, Eckly A, Freund JN, Duluc I, Gachet C, Lanza F, Leon C. Broader expression of the mouse platelet factor 4-cre transgene beyond the megakaryocyte lineage. *J Thromb Haemost*. 2015;13:115–125. doi: 10.1111/jth.12784
8. Sacco A, Bruno A, Contursi A, Dovizio M, Tacconelli S, Ricciotti E, Guillem-Llobat P, Salvatore T, Di Francesco L, Fullone R, et al. Platelet-specific deletion of cyclooxygenase-1 ameliorates dextran sulfate sodium-induced colitis in mice. *J Pharmacol Exp Ther*. 2019;370:416–426. doi: 10.1124/jpet.119.259382
9. Crescente M, Armstrong PC, Kirkby NS, Edin ML, Chan MV, Lih FB, Jiao J, Maffucci T, Allan HE, Mein CA, et al. Profiling the eicosanoid networks that underlie the anti- and pro-thrombotic effects of aspirin. *FASEB J*. 2020;34:10027–10040. doi: 10.1096/fj.202000312R
10. Gollomp K, Poncz M. Gp1ba-Cre or Pf4-Cre: pick your poison. *Blood*. 2019;133:287–288. doi: 10.1182/blood-2018-11-887513
11. Spindler M, Mott K, Schulze H, Bender M. Rapid isolation of mature murine primary megakaryocytes by size exclusion via filtration. *Platelets*. 2023;34:2192289. doi: 10.1080/09537104.2023.2192289
12. Chan MV, Armstrong PC, Papalia F, Kirkby NS, Warner TD. Optical multichannel (optimul) platelet aggregometry in 96-well plates as an additional method of platelet reactivity testing. *Platelets*. 2011;22:485–494. doi: 10.3109/09537104.2011.592958
13. Song WL, Lawson JA, Wang M, Zou H, FitzGerald GA. Noninvasive assessment of the role of cyclooxygenases in cardiovascular health: a detailed HPLC/MS/MS method. *Methods Enzymol*. 2007;433:51–72. doi: 10.1016/S0076-6879(07)33003-6
14. FitzGerald GA, Pedersen AK, Patrono C. Analysis of prostacyclin and thromboxane biosynthesis in cardiovascular disease. *Circulation*. 1983;67:1174–1177. doi: 10.1161/01.cir.67.6.1174
15. Meng H, Sengupta A, Ricciotti E, Mrcela A, Mathew D, Mazaleuskaya LL, Ghosh S, Brooks TG, Turner AP, Schanoski AS, et al. Deep phenotyping of the lipidomic response in COVID-19 and non-COVID-19 sepsis. *Clin Transl Med*. 2023;13:e1440. doi: 10.1002/ctm2.1440
16. Tang SY, Monslow J, Grant GR, Todd L, Pawelzik SC, Chen L, Lawson J, Pure E, FitzGerald GA. Cardiovascular consequences of prostanoid I receptor deletion in microsomal prostaglandin E synthase-1-deficient hyperlipidemic mice. *Circulation*. 2016;134:328–338. doi: 10.1161/CIRCULATIONAHA.116.022308
17. Yu Y, Ricciotti E, Scalia R, Tang SY, Grant G, Yu Z, Landesberg G, Crichton I, Wu W, Pure E, et al. Vascular COX-2 modulates blood pressure and thrombosis in mice. *Sci Transl Med*. 2012;4:132ra54. doi: 10.1126/scitranslmed.3003787
18. Wolock SL, Lopez R, Klein AM. Scrublet: computational identification of cell doublets in single-cell transcriptomic data. *Cell Syst*. 2019;8:281–291.e9. doi: 10.1016/j.cels.2018.11.005
19. Lopez R, Regier J, Cole MB, Jordan MI, Yosef N. Deep generative modeling for single-cell transcriptomics. *Nat Methods*. 2018;15:1053–1058. doi: 10.1038/s41592-018-0229-2
20. Traag VA, Waltman L, van Eck NJ. From Louvain to Leiden: guaranteeing well-connected communities. *Sci Rep*. 2019;9:5233. doi: 10.1038/s41598-019-41695-z
21. Rhoades SD, Weljie AM. Comprehensive optimization of LC-MS metabolomics methods using design of experiments (COLMeD). *Metabolomics*. 2016;12:183. doi: 10.1007/s11306-016-1132-4
22. Dieterle F, Ross A, Schlotterbeck G, Senn H. Probabilistic quotient normalization as robust method to account for dilution of complex biological mixtures. Application in 1H NMR metabonomics. *Anal Chem*. 2006;78:4281–4290. doi: 10.1021/ac051632c
23. Zhang Y, Da Silva JR, Reilly M, Billheimer JT, Rothblat GH, Rader DJ. Hepatic expression of scavenger receptor class B type I (SR-BI) is a positive regulator of macrophage reverse cholesterol transport in vivo. *J Clin Invest*. 2005;115:2870–2874. doi: 10.1172/JCI25327
24. Wang X, Collins HL, Ranalletta M, Fuki IV, Billheimer JT, Rothblat GH, Tall AR, Rader DJ. Macrophage ABCA1 and ABCG1, but not SR-BI, promote macrophage reverse cholesterol transport in vivo. *J Clin Invest*. 2007;117:2216–2224. doi: 10.1172/JCI32057
25. Pan H, Xue C, Auerbach BJ, Fan J, Bashore AC, Cui J, Yang DY, Trignano SB, Liu W, Shi J, et al. Single-cell genomics reveals a novel cell state during smooth muscle cell phenotypic switching and potential therapeutic targets for atherosclerosis in mouse and human. *Circulation*. 2020;142:2060–2075. doi: 10.1161/CIRCULATIONAHA.120.048378
26. Wang Y, Nanda V, Direnzo D, Ye J, Xiao S, Kojima Y, Howe KL, Jarr KU, Flores AM, Tsantilas P, et al. Clonally expanding smooth muscle cells promote atherosclerosis by escaping efferocytosis and activating the complement cascade. *Proc Natl Acad Sci USA*. 2020;117:15818–15826. doi: 10.1073/pnas.2006348117
27. Shankman LS, Gomez D, Cherepanova OA, Salmon M, Alencar GF, Haskins RM, Swiatlowska P, Newman AA, Greene ES, Straub AC, et al. KLF4-dependent phenotypic modulation of smooth muscle cells has a key role in atherosclerotic plaque pathogenesis. *Nat Med*. 2015;21:628–637. doi: 10.1038/nm.3866
28. Bennett MR, Sinha S, Owens GK. Vascular smooth muscle cells in atherosclerosis. *Circ Res*. 2016;118:692–702. doi: 10.1161/CIRCRESAHA.115.306361
29. Barrett TJ. Macrophages in atherosclerosis regression. *Arterioscler Thromb Vasc Biol*. 2020;40:20–33. doi: 10.1161/ATVBAHA.119.312802
30. Pratico D, Tillmann C, Zhang ZB, Li H, FitzGerald GA. Acceleration of atherogenesis by COX-1-dependent prostanoid formation in low density lipoprotein receptor knockout mice. *Proc Natl Acad Sci USA*. 2001;98:3358–3363. doi: 10.1073/pnas.061607398
31. Cheng Y, Wang M, Yu Y, Lawson J, Funk CD, Fitzgerald GA. Cyclooxygenases, microsomal prostaglandin E synthase-1, and cardiovascular function. *J Clin Invest*. 2006;116:1391–1399. doi: 10.1172/JCI27540
32. FitzGerald GA, Smith B, Pedersen AK, Brash AR. Increased prostacyclin biosynthesis in patients with severe atherosclerosis and platelet activation. *N Engl J Med*. 1984;310:1065–1068. doi: 10.1056/NEJM198404263101701

33. Mitchell JA, Shala F, Elghazouli Y, Warner TD, Gaston-Massuet C, Crescente M, Armstrong PC, Herschman HR, Kirkby NS. Cell-specific gene deletion reveals the antithrombotic function of COX1 and explains the vascular COX1/prostacyclin paradox. *Circ Res*. 2019;125:847–854. doi: 10.1161/CIRCRESAHA.119.314927
34. Cheng Y, Austin SC, Rocca B, Koller BH, Coffman TM, Grosser T, Lawson JA, FitzGerald GA. Role of prostacyclin in the cardiovascular response to thromboxane A2. *Science*. 2002;296:539–541. doi: 10.1126/science.1068711
35. Catella F, FitzGerald GA. Paired analysis of urinary thromboxane B2 metabolites in humans. *Thromb Res*. 1987;47:647–656. doi: 10.1016/0049-3848(87)90103-4
36. Egan KM, Lawson JA, Fries S, Koller B, Rader DJ, Smyth EM, Fitzgerald GA. COX-2-derived prostacyclin confers atheroprotection on female mice. *Science*. 2004;306:1954–1957. doi: 10.1126/science.1103333
37. Ricciotti E, FitzGerald GA. Prostaglandins and inflammation. *Arterioscler Thromb Vasc Biol*. 2011;31:986–1000. doi: 10.1161/ATVBAHA.110.207449
38. Cyrus T, Sung S, Zhao L, Funk CD, Tang S, Pratico D. Effect of low-dose aspirin on vascular inflammation, plaque stability, and atherogenesis in low-density lipoprotein receptor-deficient mice. *Circulation*. 2002;106:1282–1287. doi: 10.1161/01.cir.0000027816.54430.96
39. Nicoletti A, Kaveri S, Caligiuri G, Bariety J, Hansson GK. Immunoglobulin treatment reduces atherosclerosis in apo E knockout mice. *J Clin Invest*. 1998;102:910–918. doi: 10.1172/JCI119892
40. Akram KM, Moyo NA, Leeming GH, Bingle L, Jasim S, Hussain S, Schorlemmer A, Kipar A, Digard P, Tripp RA, et al. An innate defense peptide BPIFA1/SPLUNC1 restricts influenza A virus infection. *Mucosal Immunol*. 2018;11:71–81. doi: 10.1038/mi.2017.45
41. Xu M, Yang W, Wang X, Nayak DK. Lung secretoglobin Scgb1a1 influences alveolar macrophage-mediated inflammation and immunity. *Front Immunol*. 2020;11:584310. doi: 10.3389/fimmu.2020.584310
42. Terasawa Y, Ladha Z, Leonard SW, Morrow JD, Newland D, Sanan D, Packer L, Traber MG, Farese RV Jr. Increased atherosclerosis in hyperlipidemic mice deficient in alpha -tocopherol transfer protein and vitamin E. *Proc Natl Acad Sci USA*. 2000;97:13830–13834. doi: 10.1073/pnas.240462697
43. O'Grady NP, Tropea M, Preas HL 2nd, Reda D, Vandivier RW, Banks SM, Suffredini AF. Detection of macrophage inflammatory protein (MIP)-1alpha and MIP-1beta during experimental endotoxemia and human sepsis. *J Infect Dis*. 1999;179:136–141. doi: 10.1086/314559
44. Ray A, Dittel BN. Isolation of mouse peritoneal cavity cells. *J Vis Exp*. 2010;35:1488. doi: 10.3791/1488